Long and Short Lipid Molecules Experience the Same Interleaflet Drag in Lipid Bilayers

Andreas Horner,[1] Sergey A. Akimov,[2,3] and Peter Pohl[1,*]

[1]*Institut für Biophysik, Johannes Kepler Universität, Gruberstrasse 40, 4020 Linz, Austria*
[2]*A. N. Frumkin Institute of Physical Chemistry and Electrochemistry, Russian Academy of Sciences, Leninskiy prospekt 31/4, Moscow 119071, Russian Federation*
[3]*National University of Science and Technology "MISiS", Leninskiy prospekt 4, Moscow 119049, Russian Federation*

(Received 3 January 2013; published 24 June 2013)

Membrane interleaflet viscosity η_e affects tether formation, phase separation into domains, cell shape changes, and budding. Contrary to the expected contribution to interleaflet coupling from interdigitation, the slide of lipid patches in opposing monolayers conferred the same value $\eta_e \approx 3 \times 10^9$ J s m^{-4} for the friction experienced by the ends of both short and long chain fluorescent lipid analogues. Consistent with the weak dependence of the translational diffusion coefficient on lipid length, the in-layer viscosity was, albeit length dependent, much smaller than η_e.

DOI: 10.1103/PhysRevLett.110.268101 PACS numbers: 87.16.dt, 87.64.kv

The ability of the two membrane leaflets to slide against each other is of utmost importance for manifold cellular processes like (i) filopodia formation in cell migration [1], (ii) tether formation for neutrophil attachment to platelets during inflammation or thrombosis [2], (iii) membrane fusion [3], or (iv) membrane budding and fission [4]. In order for signaling platforms, so-called rafts to emerge, sterol and sphingolipid enriched domains must align in the two membrane monolayers [5]. Experiments on lipid bilayers suggest that such alignment is stabilized by a yet unidentified coupling mechanism. For example, lipid mixture in one leaflet of asymmetric lipid bilayers may induce the formation of registered clusters on the other leaflet, though it contains lipids which would not phase separate in a symmetric bilayer [6]. Finally, lipid interactions at the membrane midplane seem to have an impact on the mobility of individual lipid molecules [7].

What actually determines how tightly the leaflets are coupled to each other or how easily they slide against each other is under debate [6,8–10]. For example, minimization of energy expenses on local curvature [11] or maximization of the free undulation energy [12] have been put forward to explain registration of ligand-induced lipid spots of higher chain orientational order in the two leaflets. Gelation of both leaflets upon binding of negatively charged particles to only one monolayer of initially homogenous fluid lipid bilayers [13] may reflect a decreased capacity of one leaflet to accommodate disorder due to binding-induced local stiffening of the other leaflet.

Lipid interdigitation [14] would provide a unifying interleaflet coupling mechanism, which could conveniently be regulated by adjusting membrane composition. This hypothesis is supported by the notion [15] that the estimated size of $0.1–10 k_B T$ nm^{-2} of the interaction energy between leaflets exhibiting fluid-fluid phase coexistence at their midplanes [16] is roughly equal to the energy penalty associated with hypothetically inhibiting chain interdigitation [17]. Unfortunately, the values thus far reported for the viscous coefficient η_e for interleaflet drag have been widely dispersed—between 2.7×10^7–2.7×10^9 J s m^{-4} for supported bilayers [18] and 1.0×10^8–2.0×10^9 J s m^4 [19,20] for tethers formed from giant vesicles. They do not allow any conclusion about the role of interdigitation.

The goal of the present Letter is to develop a steady state assay for determining η_e in unsupported bilayers in order (i) to clarify the contribution of interdigidation to η_e and (ii) to understand whether η_e is a major determinant of the lipid diffusion coefficient D_L. Therefore, we derived two η_e from the D_L values of two different dyes (Fig. 1), one (18C atoms, 1, 1′-dioctadecyl-3,3,3′,3′-tetramethylindodicarbo-cyanine-5, 5′-disulfonic acid or 3,3′-Dioctadecyl-5,5′-Di(4-Sulfophenyl) oxacarbocyanine, DilC or DioC, Invitrogen, Carlsbad, USA) longer than the surrounding lipids (16 C atoms), and one significantly shorter (12 C atoms, (dodecyl-methylamino-sulfopropyl)-methyl-3-hydroxyflavone, F2N12S, a kind gift from A. Klymchenko, Strasbourg, France). We measured D_L in the middle of almost solvent-free horizontal lipid bilayers. They folded spontaneously in an aperture (diameter 100 μm) of a Teflon septum upon submersion beneath the air-water interface, which was covered with diphytanoylphosphatidylglycerol (DPhPG, Avanti Polar Lipids, Alabama, USA) monolayers [21,22]. The organic solvent (hexadecane/hexane, volume ratio 1:199) used for septum pretreatment is restricted to the membrane torus. F2N12S was excited at 458 nm, DioC at 488 nm, and DilC at 633 nm. Dye diffusion in and out of the confocal plane of our fluorescence correlation spectrometer (ConfoCor 3) attached to a laser scanning microscope (LSM510, both Carl Zeiss Jena, Germany) gave rise to fluorescence intensity fluctuations over time. Fitting the respective autocorrelation function to a standard two-dimensional diffusion equation [23] revealed D_L of 7.63 ± 0.81 or 11.8 ± 1.79 μm^2/s for the longer and shorter dyes.

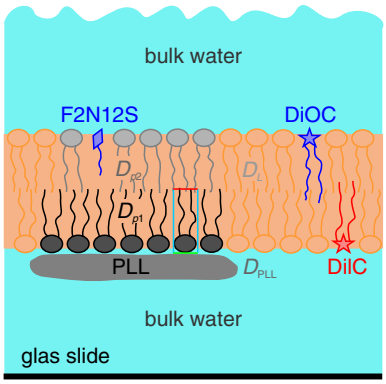

FIG. 1 (color online). Schematic representation of the membrane with adsorbed PLL. Bulk water is above and below the membrane suspended in an aperture of a Teflon septum. D_L, D_{p1}, D_{p2}, and D_{PLL} denote the dye diffusion coefficients in the absence of PLL (light orange), in contact with PLL (black lipids), in the distant monolayer of a PLL-covered patch (dark gray lipids), and the PLL diffusion coefficient in the membrane-bound state, respectively. Viscosities η are acting at the side surface (blue) of the cylindrical dye molecule (η_s), at its bottom surface (η_e) (red) and below the adsorbed PLL ($\eta_e{}^0$) (green). Molecules with longer acyl chains (red dye: DilC, blue dye: DioC) may experience a larger interfacial drag than molecules with shorter acyl chains (blue: F2N12S).

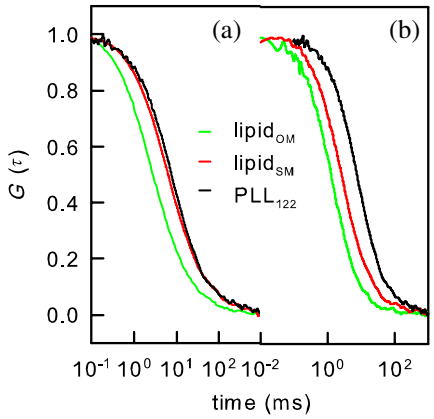

FIG. 2 (color online). Representative autocorrelation curves. Labeled PLL molecules containing 122 lysine residues [PLL_{122}(Atto488)] and unlabeled PLL_{122} ($\approx 90\%$) were added in saturating concentrations into the bulk (> 5 μg/ml) to ensure maximal coverage of the lipid bilayer. (a) In separate experiments, the long-labeled lipid analogues DilC or DioC were incorporated either into the upper leaflet (green or light gray curve) or into the lower leaflet (red or gray curve). Those in the monolayer distant to PLL_{122} (black curve) were much faster than those directly underneath it (red or gray curve). (b) The short-labeled lipid analogue (F2N12S) showed similar diffusion behavior, but at a faster rate. In this case PLL_{122} mobility was significantly slower than F2N12S in the adjacent leaflet.

We calibrated the device by using rhodamine-6G, which has a known diffusion coefficient of 426 $\mu m^2\,s^{-1}$ in solution [24].

Dissecting the contributions of the in-layer viscosity, η_s, and intermonolayer viscosity, η_e, to D_L requires that the monolayers, at least in part, slide past each other. We forced such conditions by adding poly-*L*-lysine (Sigma-Aldrich, St. Louis, USA, average molecular weight of 58 900, 25 500, 10 500, 4200 with 282, 122, 50, 20 lysine residues, respectively) into the lower compartment. PLL was labeled with Atto488 (Atto-Tec, Siegen, Germany) [PLL(Atto488)] as previously described [25]. The fraction of unlabeled PLL (initially 1:3) was increased with the total PLL concentration to ensure a constant number of labeled molecules in the focal plane. Upon binding to charged lipids, PLL(Atto488) reduces their mobility [12], because the ordering of lipids in direct contact with the polymer increases [26,27]. PLL (Atto488) may exchange its binding partners quite rapidly, so it maintains a mobility different from that of the lipids underneath [12,28].

First, autocorrelation analysis confirmed membrane binding of labeled PLL containing 122 residues [PLL_{122}(Atto488)], by showing an increase of residence time $\tau_{R,PLL}$ in the focus from ≈ 60 μs (free Atto488) to 6.6 ms. It corresponds to a two-dimensional diffusion constant D_{PLL} of 1.48 ± 0.96 $\mu m^2\,s^{-1}$ (Fig. 2, black curve). D_{PLL} depended on the total concentration of both labeled and unlabeled PLL_{122} in solution. Thus, below saturating concentrations of 5 μg/ml, D_{PLL} was larger than at higher PLL concentrations (Fig. 3, black dots).

Second, we observed that saturating PLL_{122}/PLL_{122} (Atto488) concentrations decreased D_L of DilC or DioC (Fig. 2, red or gray curve) to the diffusion coefficient $D_{SM} = 1.68 \pm 0.22$ $\mu m^2/s$ (Fig. 3, red or gray dots), which characterizes the observed average lipid mobility

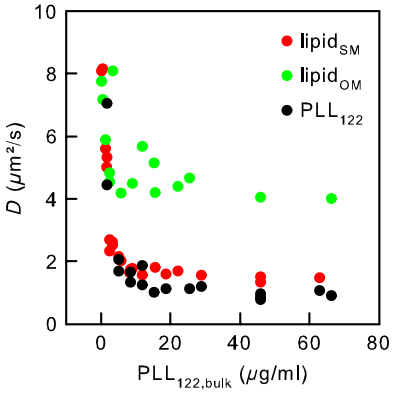

FIG. 3 (color online). Dependence of PLL_{122}'s diffusion coefficients (black dots) and labeled lipids on PLL_{122} bulk concentration. The subscripts "SM" (red or gray dots) or "OM" (green or light gray dots) denote that diffusion was monitored in the leaflet just beneath PLL or in the distant leaflet, respectively. DilC and DioC were used as lipid labels. For each data point, 5×30 sec FCS recordings were taken. The buffer contained 25 mM KCl, 10 mM HEPES, and 0.1 mM EDTA (*p*H 7).

in the adjacent monolayer. By changing the dye location to the distant leaflet (with respect to PLL) (Fig. 2, green or light gray curve), we observed a weaker PLL_{122}/PLL_{122}(Atto488) effect. That is, D_L of DilC or DioC dropped to $D_{OM} = 4.87 \pm 1.17\ \mu m^2/s$, which stands for the observed average diffusion coefficient in the distant monolayer. The difference between D_{SM} and D_{OM} confirmed that lipids from both monolayers slide past each other. Thus we have demonstrated the necessary condition for using the putative chain-length dependence of η_e to draw conclusions about the relevance of interdigitation to interleaflet coupling.

However, in addition to allowing η_e determination, PLL_{122}(Atto488) may also alter η_e via its partial lipid ordering effect. This ordering effect should depend on (i) the covered area fraction α and (ii) the size of the polymer. Unfortunately, it was impossible to determine α by FCS because unlabeled PLL displaced PLL(Atto488) bound to the membrane at higher concentrations resulting in an underestimation of PLL surface concentration. Since FCS does not adequately resolve more than ~90 particles per confocal volume, we were restricted to mobility measurements. However, the limiting surface coverage of PLL is known to be ~55% [29,30].

Substituting PLL_{122} for PLLs with chain lengths of 20, 50, and 282 residues did not change D_L at PLL bulk concentrations $<1\ \mu g/ml$, whereas D_{PLL} showed a linear length dependence. At this concentration, PLL_{20} was faster than D_{SM} [Fig. 4(a)]. At saturating concentrations of PLL_{50} and PLL_{122} ($>5\ \mu g/ml$), D_{PLL} was roughly equal to D_{SM},

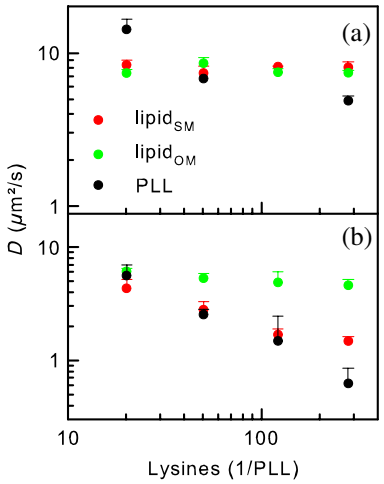

FIG. 4 (color online). The effect of PLL size on lipid mobility. PLL-induced slowdown of lipid motion is shown in the adjacent lipid monolayer (red or gray dots) and the opposite lipid monolayer (green or light gray dots). PLL's diffusion coefficients are shown in black. (a) PLL bulk concentration between 0 and 1 $\mu g/ml$. (b) Saturating PLL bulk concentration ($>5\ \mu g/ml$). Each dot drawn in the graph is an average of <16 independent measurements (compare Fig. 2). The error bars are calculated as standard deviations. Data points with missing error bars are taken from single experiments.

whereas our data showed $D_{PLL} < D_{SM}$ for PLL_{282} (Fig. 4). The diffusion coefficients are summarized in Table I.

We developed a model (see Supplemental Material [31]) to numerically calculate η_e and η_s as well as the viscosity coefficient ${\eta_e}^0$ between lipids just under the adsorbed PLL and PLL from the mobility data in Table I. Membrane-bound PLL induces a patch of ordered lipids in the adjacent monolayer. When this patch moves, it drags lipids of the opposite monolayer. The total friction of the dye within such a patch below the adsorbed PLL (Fig. 1, black lipids) can be divided into friction (i) with lipids, which are in the monolayer adjacent to PLL, (ii) with lipids, which are in the opposite monolayer, and (iii) with PLL. PLL friction with the aqueous solution is much smaller than with lipids and thus can be neglected.

To account for the inhomogeneous dye distribution β between the PLL-covered area and the PLL-free part of the monolayer, we calculate the exact diffusion coefficients of molecules within the cluster D_{p1} and D_{p2} (Fig. 1) from D_{SM} and D_{OM}:

$$\sqrt{D_{SM}} = \alpha\beta\sqrt{D_{p1}} + (1 - \alpha\beta)\sqrt{D_L}, \tag{1}$$

$$\sqrt{D_{OM}} = \alpha\beta\sqrt{D_{p2}} + (1 - \alpha\beta)\sqrt{D_L}. \tag{2}$$

The dependence of D_{p1} and D_{p2} from the relevant viscosity coefficients η_e, ${\eta_e}^0$, and η_s according to the Einstein-Smoluchowski relation leads to six unknown values (η_e, η_s, ${\eta_e}^0$, D_{p1}, D_{p2}, β) and six equations which we numerically solved. This calculation assumes that the lipids in the area that is not covered by PLL may be characterized by D_L, i.e., that they retain the mobility measured in the absence of PLL. D_{p1} and D_{p2} are linked via η_e and η_s:

$$D_{p2} = \frac{k_B T}{\eta_s S_s + \frac{k_B T}{D_{p1} + k_B T/\eta_e S_e}}, \tag{3}$$

where S_s and S_e denote the side and bottom surfaces of the presumably cylindrical-shaped labeled lipids ($S_s = 2\pi RH$, $S_e = \pi R^2$, where H and R are the height and the radius of the cylinder, respectively).

The encouraging result of the calculation was that $\eta_e = (3.0 \pm 0.8) \times 10^9\ J\,s\,m^{-4}$ did not depend on PLL size, indicating that PLL had a negligible effect on the intermonolayer drag. Since α was an estimate from literature values, we tested the effect of its underestimation on η_e. Our calculations revealed that higher values for α did not alter η_e at all (see Supplemental Material [31]).

Equation (3) assumes that the contributions of η_s and η_e can be considered independently. However, η_s serves to accelerate the lipids in contact with the dragged label. In turn, these lipids must contribute to η_e. If the six nearest neighbors move with the same velocity as the label, η_e is equal to $1.5 \times 10^9\ J\,s\,m^{-4}$. This result represents the upper

TABLE I. Diffusion coefficients (D), interlayer (η_e), and in-layer viscosities (η_s) of long (DilC, DioC, denoted as l) and short lipid dyes (F2N12S, denoted as s) in free-standing lipid membranes formed of DPhPG. PLL was added in saturating concentrations into the bulk ($> 5\ \mu$g/ml) to ensure maximal coverage of the lipid bilayer ($\sim 55\%$). n indicates the number of lysine residues per macromolecule. D_L, D_{SM}, D_{OM}, and D_{PLL} denote the dye diffusion coefficients in the absence of PLL, with PLL bound to the labeled leaflet, with PLL bound to the unlabeled leaflet, and the PLL diffusion coefficient in the membrane bound state, respectively. The label distribution between the membrane areas covered by PLL and free of PLL are indicated by $\beta = x_{domain}/x_{surround}$. The errors are calculated as standard deviations.

Dye	n	D_L ($\mu m^2/s$)	D_{SM} ($\mu m^2/s$)	D_{OM} ($\mu m^2/s$)	D_{PLL} ($\mu m^2/s$)	η_e (10^9 J s m^4)	η_s (10^9 J s m^4)	β
l	20	7.6 ± 1.1	4.3 ± 0.9	6.1 ± 0.4	5.6 ± 1.3	3 ± 2.1	0.15 ± 0.09	1.4 ± 0.6
l	50	7.8 ± 1	2.8 ± 0.5	5.3 ± 0.6	2.5 ± 0.3	3.1 ± 1.3	0.14 ± 0.06	1.5 ± 0.2
l	122	7.6 ± 0.8	1.7 ± 0.2	4.9 ± 1.2	1.5 ± 1	2.7 ± 1.7	0.16 ± 0.07	1.7 ± 0.4
s	122	11.8 ± 1.8	4 ± 0.3	7.1 ± 0.6	1.5 ± 1	3.1 ± 1	0.11 ± 0.05	1.2 ± 0.2
l	282	7.7 ± 1.8	1.5 ± 0.2	4.6 ± 0.6	0.6 ± 0.2	3.1 ± 1.1	0.14 ± 0.08	1.4 ± 0.1

limit of these "edge effects." For the more realistic estimate of ~ 1.2 nm^2 for the incremental area, η_e amounts to 2.2×10^9 J s m^{-4}. That is, the η_e values calculated with and without edge effects do not significantly differ from each other indicating that the edge effects may be neglected.

Finally, we measured η_e and η_s with the short dye F2N12S. Since the size of the polymers appeared to be irrelevant, we only used PLL_{122} and PLL_{122}(Atto488) to induce the slide of monolayer patches past each other. η_s amounted to only 2/3 of the value measured with DilC/DioC which nicely corresponds to the ratio of the dye's hydrophobic lengths. The smaller η_s may have also reflected the different ratio of head-to-tail cross-sectional areas. Contrary to the intuitive reasoning, $\eta_e = 3.0 \pm 0.8 \times 10^9$ J s m^{-4} was similar to the η_e for long dyes (Table I).

The similarity in η_e for both dyes suggests that frictional forces on the end of a chain, regardless of length, will primarily reflect interactions with chain segments in the same leaflet. This agrees well with high acyl chain dynamics found in NMR studies of bilayers with significant chainlength mismatch: Although the methylene groups of the longer acyl chains penetrate, on average, across the bilayer midplane, they are highly disordered and their mobility is not significantly constrained by interaction with the opposite leaflet [32]. Our result is also in line with a number of experimental and modeling studies that have shown a high propensity for acyl chain backfolding, i.e., a significant probability of finding the methyl group of a given chain close to the headgroup region of the same leaflet [33].

Thus, the unordered chain's ends are exposed to a much "rougher" environment than the lipid side surfaces, especially if compared to the "smooth" side surfaces in the ordered regions close to the lipid headgroups. This might explain why η_s is about an order of magnitude smaller than η_e (Table I). From (i) $\eta_s \ll \eta_e$ and (ii) the independence of η_e on the acyl chain length L follows that the continuum fluid hydrodynamic model for diffusion in membranes [34] must fail to correctly predict the dependence of D_L on L. That is, we are able to confirm a prediction from a 30 years old systematic study of lipid diffusion [7] that the strong friction at membrane midplane accounts for the deviations from the inverse proportionality $D_L \sim 1/L$.

The similarity in η_e for both the short dye F2N12S and the long dyes DilC/DioC rules out interdigitation as a coupling mechanism. This result is in line with the observation that cholesterol reduces the extent of chain interdigitation [35] albeit promoting raft formation. It also agrees with the conclusion made from the observed similarity of the diffusion coefficients of (i) a lipid probe containing both a short (10 C atoms) and a long acyl chain (18 C atoms) and (ii) a lipid probe with two identical acyl chains of average length (14 C atoms) [36].

In contrast to previous η_e measurements by the microaspiration technique, our fluorescence measurements were performed in the steady state. We thus avoided possible effects that the speed of the tether pulling from giant vesicles may have on η_e. The broad scattering of the microaspiration η_e values had thus far made it impossible to rule out that possibility [37]. Our approach originated from attempts to derive η_e from the diffusion of lipid dyes on solid supported membranes [18]. We now substituted the solid support for comparatively small PLL molecules, which locally reduced the diffusional mobility. The resulting value for η_e is in good agreement with the value of 2×10^9 J s m^{-4} derived from the pH-triggered ejection of a tubule out of giant vesicles [20]. Since these experiments were carried out with unsaturated unbranched lipids and ours with saturated branched lipids, the lipid composition is unlikely to be responsible for the difference to the previously derived values which are one or 2 orders of magnitude smaller [19,37].

We conclude (i) that η_e is the major determinant of lipid mobility and that (ii) interleaflet coupling is not due to interdigitation. The impact of local differences in interleaflet drag for domain registration should depend on the absolute interaction energy. Experiments are underway for its determination.

This work was supported by the Upper Austrian government. We thank Andrey S. Klymchenko (Université de Strasbourg, Laboratoire de Biophotonique

et Pharmacologie, France) for kindly providing F2N12S. S. A. A. was supported by the Federal Targeted Program "Scientific and scientific-pedagogical personnel of the innovative Russia" 2009-2013" (state contracts 8166, 14.740.11.1409, theme 3400022); Program of Creation and Development of National University of Science and Technology "MISiS"; Russian Foundation for Basic Research (Grants No. 12-04-01426, No. 12-04-31466, and No. 11-04-01001), Program of Presidium of Russian Academy of Sciences "Molecular and Cell Biology."

*peter.pohl@jku.at

[1] D. A. Lauffenburger and A. F. Horwitz, Cell **84**, 359 (1996).
[2] D. W. Schmidtke and S. L. Diamond, J. Cell Biol. **149**, 719 (2000).
[3] R. Jahn and R. H. Scheller, Nat. Rev. Mol. Cell Biol. **7**, 631 (2006).
[4] G. van Meer, D. R. Voelker, and G. W. Feigenson, Nat. Rev. Mol. Cell Biol. **9**, 112 (2008).
[5] P. F. Devaux and R. Morris, Traffic **5**, 241 (2004).
[6] M. D. Collins and S. L. Keller, Proc. Natl. Acad. Sci. U.S.A. **105**, 124 (2008).
[7] W. L. Vaz, R. M. Clegg, and D. Hallmann, Biochemistry **24**, 781 (1985).
[8] T. Baumgart, S. T. Hess, and W. W. Webb, Nature (London) **425**, 821 (2003).
[9] H. J. Risselada and S. J. Marrink, Proc. Natl. Acad. Sci. U.S.A. **105**, 17 367 (2008).
[10] S. Chiantia, P. Schwille, A. S. Klymchenko, and E. London, Biophys. J. **100**, L1 (2011).
[11] D. A. Pantano, P. B. Moore, M. L. Klein, and D. E. Discher, Soft Matter **7**, 8182 (2011).
[12] A. Horner, Y. N. Antonenko, and P. Pohl, Biophys. J. **96**, 2689 (2009).
[13] B. Wang, L. Zhang, S. C. Bae, and S. Granick, Proc. Natl. Acad. Sci. U.S.A. **105**, 18 171 (2008).
[14] J. L. Slater and C. Huang, Prog. Lipid Res. **27**, 325 (1988).
[15] S. May, Soft Matter **5**, 3148 (2009).
[16] M. D. Collins, Biophys. J. **94**, L32 (2008).
[17] I. Szleifer, A. Ben-Shaul, and W. M. Gelbart, J. Phys. Chem. **94**, 5081 (1990).
[18] R. Merkel, E. Sackmann, and E. Evans, J. Phys. (Les Ulis) **50**, 1535 (1989).
[19] E. Evans and A. Yeung, Chem. Phys. Lipids **73**, 39 (1994).
[20] J. B. Fournier, N. Khalifat, N. Puff, and M. I. Angelova, Phys. Rev. Lett. **102**, 018102 (2009).
[21] S. Serowy, S. M. Saparov, Y. N. Antonenko, W. Kozlovsky, V. Hagen, and P. Pohl, Biophys. J. **84**, 1031 (2003).
[22] A. Springer, V. Hagen, D. A. Cherepanov, Y. N. Antonenko, and P. Pohl, Proc. Natl. Acad. Sci. U.S.A. **108**, 14 461 (2011).
[23] D. Magde, E. Elson, and W. W. Webb, Phys. Rev. Lett. **29**, 705 (1972).
[24] Z. Petrasek and P. Schwille, Biophys. J. **94**, 1437 (2008).
[25] Y. N. Antonenko, A. Horner, and P. Pohl, PLoS ONE **7**, e52839 (2012).
[26] C. Schwieger and A. Blume, Eur. Biophys. J. **36**, 437 (2007).
[27] G. Forster, C. Schwieger, F. Faber, T. Weber, and A. Blume, Eur. Biophys. J. **36**, 425 (2007).
[28] U. Golebiewska, A. Gambhir, G. Hangyás-Mihályné, I. Zaitseva, J. Rädler, and S. McLaughlin, Biophys. J. **91**, 588 (2006).
[29] D. Volodkin, V. Ball, P. Schaaf, J.-C. Voegel, and H. Mohwald, Biochim. Biophys. Acta, Biomembr. **1768**, 280 (2007).
[30] J. H. Kleinschmidt and D. Marsh, Biophys. J. **73**, 2546 (1997).
[31] See Supplemental Material at http://link.aps.org/supplemental/10.1103/PhysRevLett.110.268101 for derivation of the model.
[32] D. Lu, I. Vavasour, and M. R. Morrow, Biophys. J. **68**, 574 (1995).
[33] Z. C. Xu and D. S. Cafiso, Biophys. J. **49**, 779 (1986).
[34] P. G. Saffman and M. Delbruck, Proc. Natl. Acad. Sci. U.S.A. **72**, 3111 (1975).
[35] T. J. McIntosh, S. A. Simon, D. Needham, and C. H. Huang, Biochemistry **31**, 2012 (1992).
[36] V. Schram and T. E. Thompson, Biophys. J. **69**, 2517 (1995).
[37] R. M. Raphael and R. E. Waugh, Biophys. J. **71**, 1374 (1996).